ELSEVIER

Journal of Chromatography A, 859 (1999) 203–219

JOURNAL OF CHROMATOGRAPHY A

www.elsevier.com/locate/chroma

Efficiency studies in nonaqueous capillary electrophoresis

Vicki L. Ward, Morteza G. Khaledi*

Department of Chemistry, Box 8204, North Carolina State University, Raleigh, NC 27695-8204, USA

Received 8 October 1998; received in revised form 29 July 1999; accepted 3 August 1999

Abstract

Nonaqueous capillary electrophoresis (NACE) is a relatively new area with several advantages that include enhanced efficiency and improved detection sensitivity. The goal of this study was to investigate the influence of NACE compared to aqueous CE on the separation efficiency of oligosaccharides. The applied voltage and buffer concentration were optimized for the aqueous and nonaqueous buffer media to minimize the band broadening effects of Joule heating and electrophoretic dispersion. At the optimized conditions a 1.5-fold enhancement in efficiency was obtained with the nonaqueous buffer medium.

Keywords: Nonaqueous capillary electrophoresis; Efficiency; Buffer composition; Oligosaccharides

1. Introduction

The high efficiency of capillary electrophoresis (CE) is a result of the plug like profile unlike pressure-driven systems (HPLC) which experience laminar flow profiles. Jorgenson and Lukacs [1] expressed the efficiency under ideal conditions where longitudinal diffusion is the only band broadening mechanism present by Eq. (1)

$$N = \frac{(\mu + \mu_{eo})V}{2D} \quad (1)$$

where μ, μ_{eo}, V and D represent the electrophoretic mobility, electroosmotic mobility, applied voltage and diffusion coefficient, respectively. Eq. (1) predicts that the efficiency will increase linearly with voltage. However, in practice there are several possible sources of band broadening that can influence the separation efficiency. These band broadening mechanisms include contributions from injection, electrophoretic dispersion, Joule heating, wall adsorption, local turbulences due to non-uniformly charged capillary walls, and hydrostatic flow [2–5]. For the most part, variances due to these band broadening phenomena can be suppressed by careful experimental design and high efficiencies can be achieved.

Local turbulences and hydrostatic flow can be minimized by thoroughly conditioning the capillary and by equally positioning as well as filling the buffer reservoirs where the capillary ends reside, respectively. To minimize injection contributions to the loss in efficiency, the injected plug length should be kept as small as possible. The rule of thumb is that the injection plug length should not exceed 1%

*Corresponding author. Tel.: +1-919-7372-545; fax: +1-919-5155-079.

E-mail address: khaledi@chemdept.chem.ncsu.edu (M.G. Khaledi)

0021-9673/99/$ – see front matter
PII: S0021-9673(99)00839-0

of the total capillary length. However, Delinger and Davis reported that the 1% injection plug is often too large in many instances and may lead to capillary overloading [6]. Electrophoretic dispersion and Joule heating can be controlled by optimizing the conductivity difference between the sample and separation buffer and by operating at a voltage where the heat can be effectively dispersed, respectively.

The goal of this study was to investigate the influence of nonaqueous capillary electrophoresis (NACE) on the separation efficiency of oligosaccharides compared to aqueous CE. The potential of NACE to enhance efficiency stems from the lower conductivities associated with nonaqueous media which in turn minimize the band broadening effects associated with Joule heating.

2. Experimental

2.1. Capillary electrophoresis system

All separations were carried out on a laboratory-made CE system with UV detection at 270 nm. The CE set-up consists of a 0–50 kV reversible high-voltage power supply (Model SL50PN30, Spellmann, Plainview, NY, USA), and a Plexiglass safety interlock box to house the high-voltage end of the capillary. The fused-silica capillary was 52 μm I.D.×365 μm O.D. (Polymicro Technologies, Tucson, AZ, USA). The total capillary length was 60 cm with an effective length of 47 cm. Temperature control was maintained at 25°C using an oil bath (Lauda K-2/R, Brinkmann Instruments, Westbury, NY, USA). Data acquisition was performed using a program written within LabView (National Instruments, Austin, TX, USA).

2.2. Reagents and chemicals

Maltose, maltotriose, maltotetraose, maltopentaose, maltohexaose and maltoheptaose oligosaccharide standards were purchased from Sigma (St. Louis, MO, USA). Anhydrous citric acid and formamide were obtained from Fluka (Buchs, Switzerland). The fluorescent tag 8-aminonaphthalene-1,3,6-trisulfonic acid (ANTS) was purchased from Molecular Probes (Eugene, OR, USA). Acetic acid, acetone, sodium hydroxide, dimethylsulfoxide (DMSO), NaH_2PO_4 and KH_2PO_4 were acquired from Fisher (Fairlawn, NJ, USA). Sodium cyanoborohydride ($NaCNBH_3$) was purchased from Aldrich (Milwaukee, WI, USA). Milli-Q deionized water was obtained in the laboratory.

2.3. Derivatization with ANTS

The ANTS derivatization procedure for the oligosaccharides was adapted from Chiesa and Horváth [7]. A 0.14 *M* ANTS solution was prepared in acetic acid–water (3:17, v/v). A 286-μl aliquot of the ANTS solution was added to an amber micro centrifuge tube already containing 100 μl of a 0.01 *M* aqueous solution of the oligosaccharide. To this mixture, 200 μl of 1 *M* $NaCNBH_3$ in DMSO was added. The centrifuge tube was then gently vortexed and placed in a 37°C water bath for 15 h. Derivatization begins with the reducing end of the saccharide reacting with the amino group of ANTS to form a Schiff base. Cyanoborohydride then reacts with the Schiff base to reduce the primary amine to a secondary. Prior to CE analysis, the derivatized samples were filtered through 0.45-μm polypropylene filters from Scientific Resources (Eatontown, NJ, USA) and diluted to the desired concentration with 18 MΩ Milli-Q water.

2.4. Procedure

The solvents used in the preparation of the aqueous and nonaqueous buffers were Milli-Q deionized water and formamide, respectively (Table 1). Acidic buffers of sodium phosphate, potassium phosphate and citric acid were prepared at a concentration of 50 m*M* with the pH adjusted to 3.5 using 1 *M* sodium

Table 1
Physical properties of the solvents (from Ref. [14])

Solvent	Viscosity (cP), 25°C	Dielectric constant	ϵ/η
Water	0.89	80	90
Formamide	3.3	111	34

hydroxide. The basic buffers consisted of sodium phosphate at concentrations of 50, 70 and 100 m*M* for the aqueous studies, and 50, 75 and 90 m*M* for the nonaqueous studies. The pH for all the buffers was adjusted to 9 with 1 *M* sodium hydroxide (in this paper pH* refers to apparent pH for the nonaqueous buffers). A water content of ca. 6% exists in the formamide buffers due to pH adjustment with aqueous 1 *M* NaOH and the solvent itself. The samples used in the acidic and basic buffer studies were ANTS-derivatized maltotriose and maltopentaose, respectively. The oligosaccharide samples were prepared at a concentration of $2.64 \cdot 10^{-4}$ *M* in Milli-Q deionized water and injected hydrodynamically. The oligosaccharide mixture consisted of maltoheptaose, maltohexaose, maltopentaose, maltotetraose, maltotriose and maltose each at a concentration of $2.64 \cdot 10^{-4}$ *M* in the mixture. Acetone was utilized as the neutral marker for all electroosmotic mobility studies and was injected hydrodynamically.

The viscosity of formamide was determined at various temperatures (25, 30, 35.5 and 40.5°C) using a Ubbelhode viscometer (Model 50F243, Cannon, State College, PA, USA). The viscometer was cleaned with filtered methanol and oven dried prior to use. A 50-ml quantity of formamide was added to the lower reservoir of the viscometer which was kept in a temperature controlled water bath (Porta Temp, Precision Scientific, Chicago, IL, USA). A pipette bulb was then used to pull the solvent through a capillary and up into a upper bulb of the viscometer. The efflux time was measured by monitoring the time it takes for the solvent meniscus to pass from one etched mark down to the next. Kinematic viscosity (Stokes) is then calculated from the viscometer data and converted to standard viscosity (Poise) by multiplying by the solvent density. Density measurements were performed at each temperature by weighing a 5 ml aliquot of the solvent in triplicate and averaging. The density of a liquid decreases as it is heated and therefore the standard viscosity decreases with increased temperature.

Capillary conditioning was performed at the beginning of each day by first rinsing with 1 *M* sodium hydroxide for 20 min followed by Milli-Q deionized water for 2 min and lastly with buffer for 20 min. Each sample was injected three times and the results were averaged.

3. Results and discussion

3.1. Effects of buffer type on conductivity and efficiency

The three aqueous buffers investigated were sodium phosphate, potassium phosphate and citric acid all at pH 3.5 in deionized water. Ohm's law plots were performed on each buffer by measuring current as a function of voltage to determine if Joule heating has occurred. Joule heating happens when the heat generated within the capillary can no longer be effectively dissipated. Heat is dissipated through the capillary walls by conduction and transferred to the surrounding air by convection and radiation. The use of small capillary diameters and forced convection such as a fan or thermostated bath provide the most efficient means of heat removal. Joule heating diminishes the efficiency by producing a parabolic flow profile within the capillary. The deviation from linearity in Fig. 1 is an indication of Joule heating in the three aqueous buffers tested. Also from this data conclusions were made about the conductivity of the different buffer systems. In Fig. 1, citric acid was the least conductive buffer followed by sodium phosphate and potassium phosphate, Ideally, one would want a buffer system with low conductivity to minimize the band broadening effects of Joule heating.

The influence of buffer type and electric field strength on efficiency in aqueous CE is demonstrated in Fig. 2. Efficiency can be enhanced by increasing the electric field strength up to a point after which Joule heating becomes a problem.

Electrophoretic dispersion is another band broadening phenomenon that produces a fronting or tailing distortion of the peak symmetry and thus a loss in efficiency. It occurs as a result of conductivity differences between the buffer and sample zones. Consequently, the two zones experience different electric field strengths which in turn leads to the peak distortions. In Fig. 2 both the sodium and potassium phosphate buffers produced similar maximum efficiencies of $253\,700 \pm 15\,500$ and $262\,000 \pm 7900$ plates, respectively, whereas the maximum efficiency for the citric buffer was $209\,000 \pm 8500$. The higher efficiencies of the phosphate buffers was attributed to the mobility of the phosphate co-ion being more

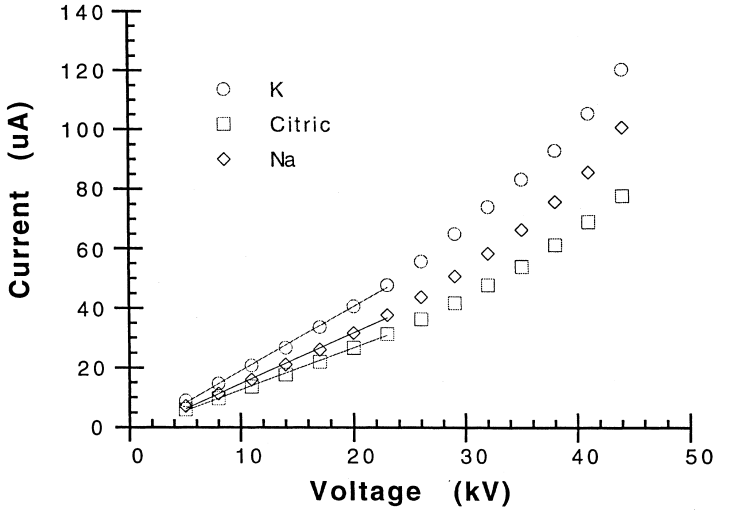

Fig. 1. Ohm's law plots for the acidic buffers in aqueous media. All three buffers are linear (0.999) out to 23 kV. Experimental conditions: 50 m*M* buffers of sodium phosphate, potassium phosphate and citric acid; pH 3.5; capillary 60 cm (effective length 47 cm)×52 μm I.D.×365 μm O.D.

closely matched to the negatively charged analyte, thereby minimizing the band broadening effects of electrophoretic dispersion.

These studies could not be carried out in formamide with the negatively charged oligosaccharide samples under acidic conditions due to long retention times. Sodium phosphate buffer at pH 9 was chosen for the remaining experiments due to the high oligosaccharide efficiencies and low conductivities observed with this buffer. Additionally, sodium phosphate (monobasic) has a high solubility in the nonaqueous solvent, formamide.

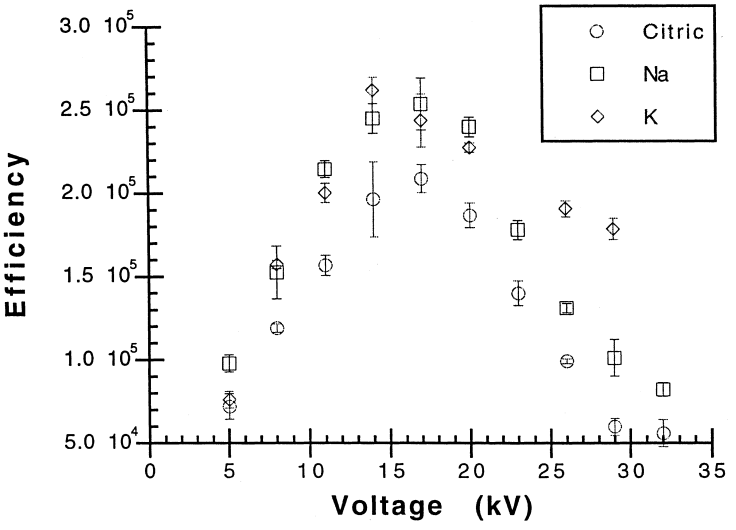

Fig. 2. Influence of aqueous buffer composition and applied voltage on the efficiency of ANTS-derivatized maltotriose in CE. Experimental conditions as in Fig. 1.

3.2. Effects of the nonaqueous medium on efficiency

Comparisons were made between NACE and aqueous CE to determine the effects of the nonaqueous solvent, formamide, on the oligosaccharide efficiency. To minimize electrophoretic dispersion and Joule heating, the buffer concentration and electric field strength were optimized, respectively. The Ohm's law plot in Fig. 3b shows that the Ohm's law is obeyed over the entire voltage range (5–45 kV) in the nonaqueous buffer, whereas for the aqueous buffers deviations from linearity begins at voltages less than 20 kV. The better linearity for the

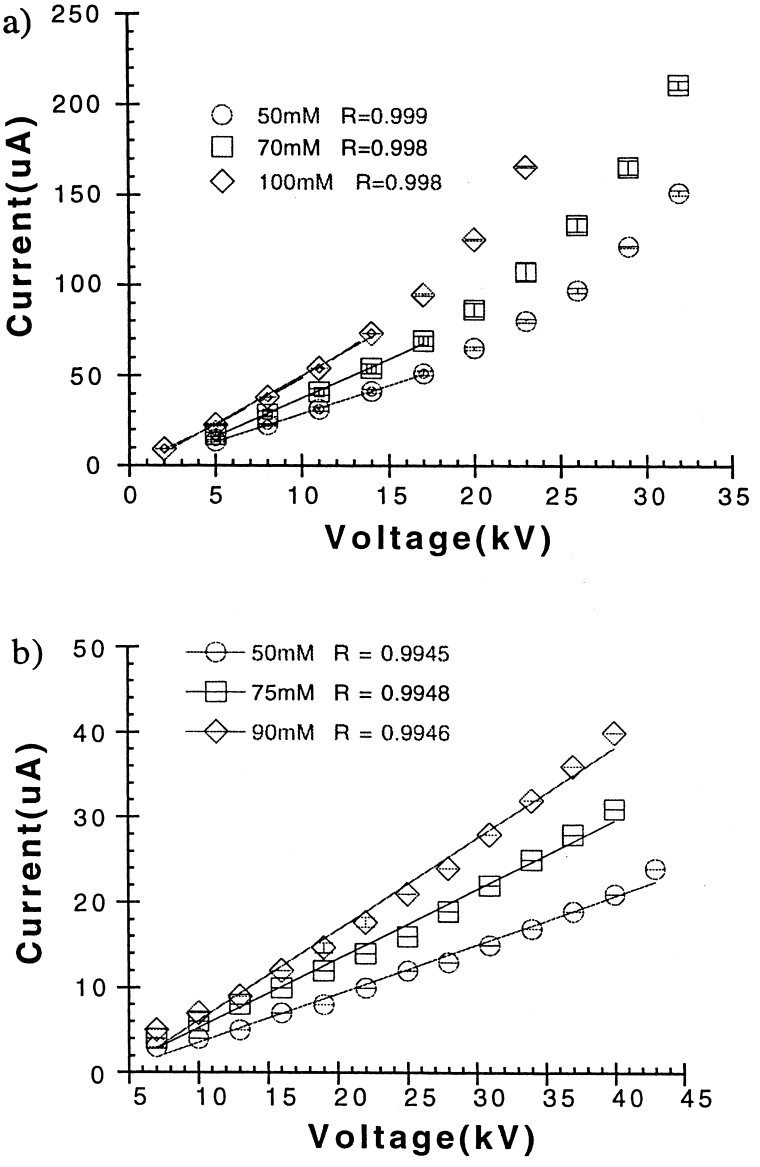

Fig. 3. Ohm's law plots for (a) aqueous CE and (b) NACE. Experimental conditions: aqueous buffers are 50, 70, 100 m*M* sodium phosphate, pH 9; nonaqueous (formamide) buffers are 50, 75 and 90 m*M* sodium phosphate, pH 9*; capillary dimensions are 60 cm (effective length 47 cm)×52 μm I.D.×365 μm O.D.

nonaqueous systems is due to the overall lower electrical currents that allow operating at higher electric field strengths and/or buffer concentrations without significant Joule heating effects.

Fig. 4a and b illustrate the effects of applied voltage and buffer concentration on efficiency for the aqueous and formamide media, respectively. The efficiencies in the nonaqueous medium were overall higher. Interestingly, the optimum conditions for the aqueous and nonaqueous systems is approximately the same. The efficiency of ANTS-derivatized maltopentaose in the nonaqueous medium was maximized at 332 000±18 000 plates with a buffer concentration of 75 m*M* and 19 kV. The aqueous buffer medium produced a maximum efficiency of 220 000±6000 plates at a 70 m*M* buffer concentration and an applied voltage of 17 kV. As expected, the maximum efficiency in the aqueous medium (Fig. 4a) was achieved at a voltage just prior to the occurrence of Joule heating as indicated by the

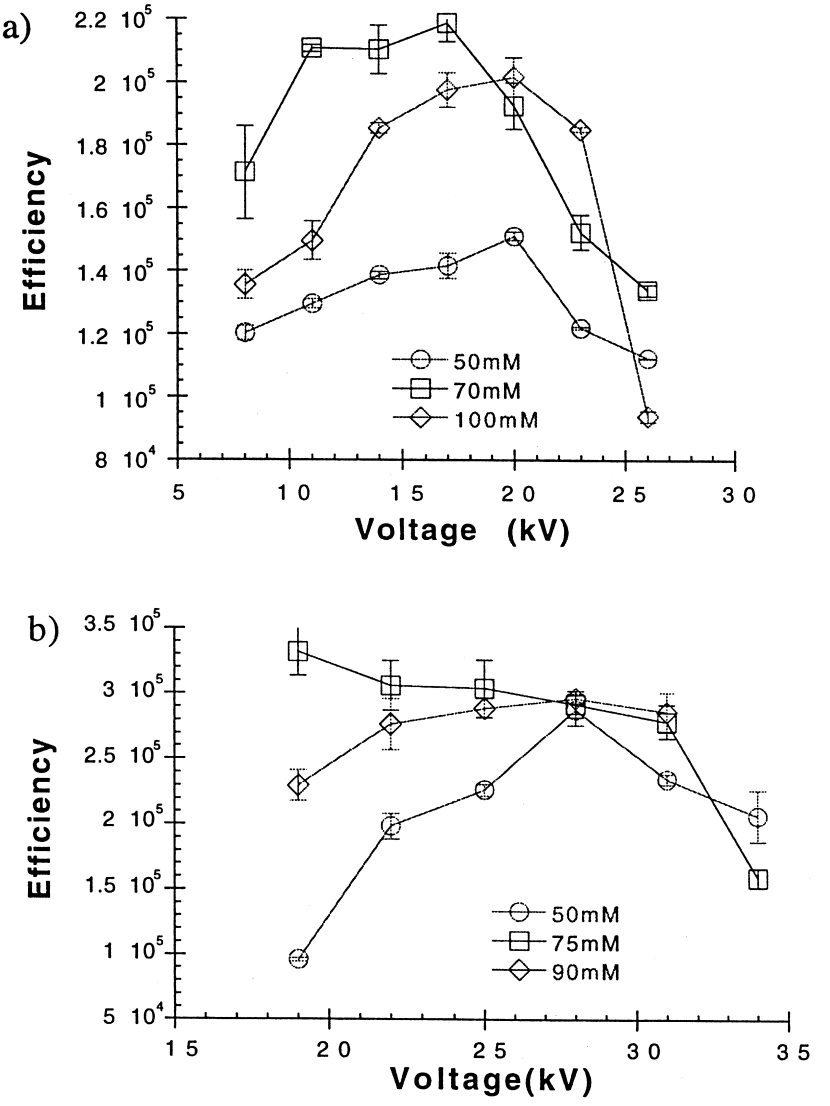

Fig. 4. Effect of buffer ionic strength and applied voltage on efficiency in (a) aqueous CE and (b) NACE. Sample is ANTS-derivatized maltopentaose ($2.64 \cdot 10^{-4}$ *M*). Experimental conditions as in Fig. 3.

Ohm's law plot in Fig. 3a. Similarly, the efficiency in the nonaqueous medium (Fig. 4b) also reaches a maximum and declines with additional increases in voltage; however, there is no indication of Joule heating according to the Ohm's law plot in the nonaqueous media (Fig. 3b). This observance suggested that Joule heating may not be the only band broadening mechanism present. However, before Joule heating could be completely ruled out in the nonaqueous buffer we first examined the accuracy by which the Joule heating was being measured. It is possible that the Ohm's law plot is not the best indicator for Joule heating in nonaqueous systems. The viscosity of liquids is more sensitive to changes in temperature; it decreases exponentially with temperature [8]. The extent of temperature effects on viscosity is not the same for all solvents. The temperature dependence of viscosity for formamide was experimentally determined by plotting measured viscosities (mPa s) versus $1/T$ in Kelvin and compared to literature values for water. From the slopes of these plots it is evident that formamide viscosity (slope = 2304) is more sensitive than water (slope = 1820) to variations in temperature. In order to get a better perspective of the heat being generated within the capillary, experiments were performed to measure the mobility of a neutral marker (acetone) as well as the internal capillary temperatures over a given voltage range for both the aqueous and nonaqueous buffers. The variations in electroosmotic mobility with electric field strength are shown in Fig. 5a and b for the different aqueous and nonaqueous buffer concentrations. In principle, μ_{eo} should be independent of the applied voltage; however, if Joule heating occurs the viscosity of the medium will decrease resulting in an increased μ_{eo} as given by Eq. (2)

$$\mu_{eo} = \frac{\epsilon\zeta}{4\pi\eta} \tag{2}$$

where ϵ, ζ and η represent the dielectric constant, zeta potential and viscosity, respectively. As expected, the higher the buffer concentration the lower the μ_{eo} values in both systems. The electroosmotic mobility increased over the voltage range of 14–41 kV (233–683 V/cm) at the nonaqueous buffer concentrations 50, 75 and 90 m*M* by 16, 21 and 28%, respectively (Fig. 5b). Aqueous buffer concentrations of 50, 70 and 100 m*M* increased μ_{eo} by 16, 21 and 32%, respectively (Fig. 5a), over the voltage range of 6–17 kV (100–283 V/cm). It is evident from the mobility data that the nonaqueous medium extends the usable voltage range considerably. Despite the increases in μ_{eo}, we do not feel that this is conclusive enough to suggest that Joule heating is the cause of the reduced efficiencies of the oligosaccharide shown in Fig. 4b. To further investigate the possibility of Joule heating, the internal capillary temperatures were calculated over the same voltage ranges for both the aqueous and nonaqueous buffer media. The viscosity and electroosmotic mobility can be related to the temperature inside the capillary by Eqs. (3), (4) and (5) [9]

$$\frac{1}{\eta} = A e^{-\frac{B}{T}} \tag{3}$$

$$\frac{\mu_{eo1}}{\mu_{eo2}} = e^{-\left(\frac{B}{T_1} - \frac{B}{T_2}\right)} \tag{4}$$

$$T_2 = \frac{B}{\ln(\mu_{eo1}) - \ln(\mu_{eo2}) + \frac{B}{T_1}} \tag{5}$$

where B is a constant representing the change in viscosity as a function of temperature, μ_{eo1} was obtained at $\leq$5 kV (where no Joule heating occurs, $T_1 = 298$ K), and μ_{eo2} is the measured electroosmotic flow (EOF) at higher voltages. The B value for water was obtained from the literature and equals 1820 [9]. The temperature dependence of the viscosity coefficient B for formamide was calculated using equations given by Skomorokhov and Dregalin [10] as well as experimentally determined using a viscometer. Comparable slopes of 2304 and 2331 were obtained with the latter being utilized in the internal capillary temperature calculations. Additionally, the experimental value of 3.3 cP at 298 K agrees with the literature value for formamide [11]. The results of the internal capillary temperature calculations are given in Fig. 6a and b. Despite the increases in mobility for acetone in the nonaqueous buffers shown in Fig. 5b, it does not seem that enough Joule heating is generated to cause the decreases in the oligosaccharide efficiencies shown in Fig. 4b. This is supported by the fact that the internal capillary

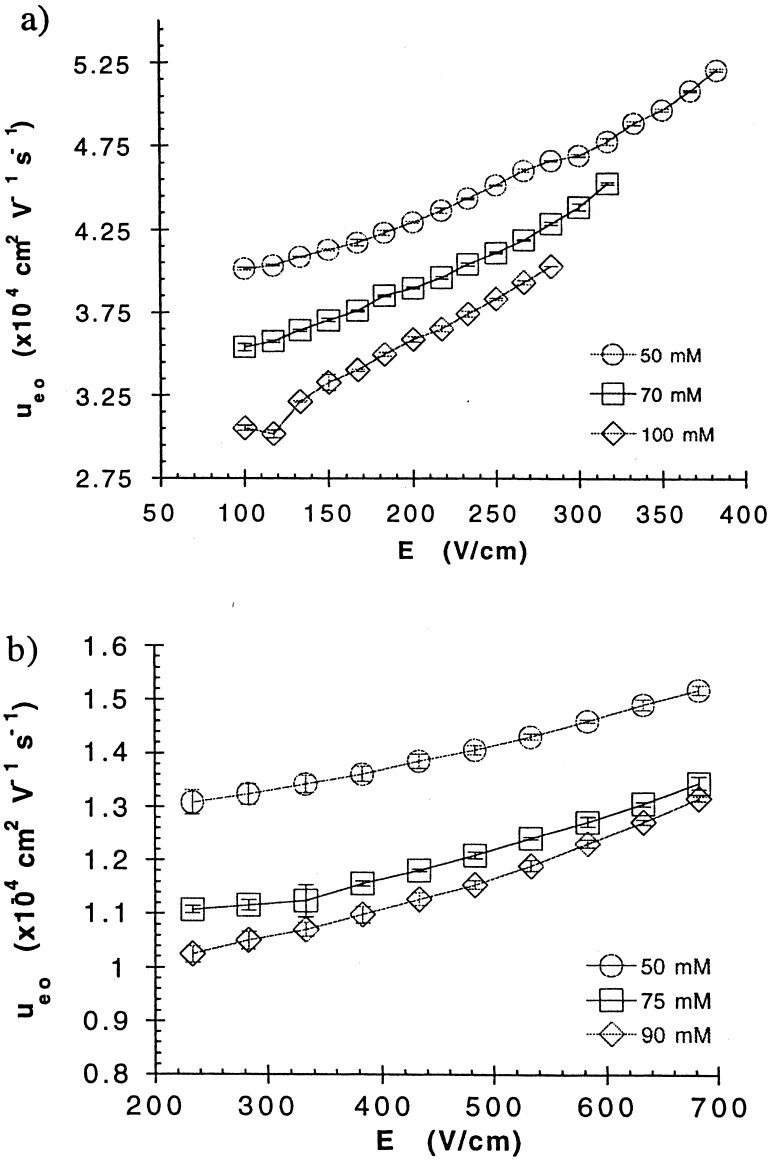

Fig. 5. Mobility of acetone as a function of applied voltage in (a) aqueous and (b) formamide. Experimental conditions and capillary dimensions as in Fig. 3.

temperatures for the nonaqueous buffers shown in Fig. 6b do not vary greatly from ambient temperature below 0.6 W. Additionally, very similar slopes were observed for the three nonaqueous buffer concentrations tested, suggesting that the heat is being dissipated. Given these results, it appears that the linearity of the nonaqueous Ohm's law plots (Fig. 3b) is an indication of efficient heat removal. The lower power levels generated by the nonaqueous buffers further demonstrates the lower conductivity advantage of the nonaqueous medium.

Fig. 6a shows the dependence of internal capillary temperature on power for the aqueous buffers. The aqueous media produced slopes which were overall higher than the nonaqueous buffers and increased with buffer concentration, all of which suggests that

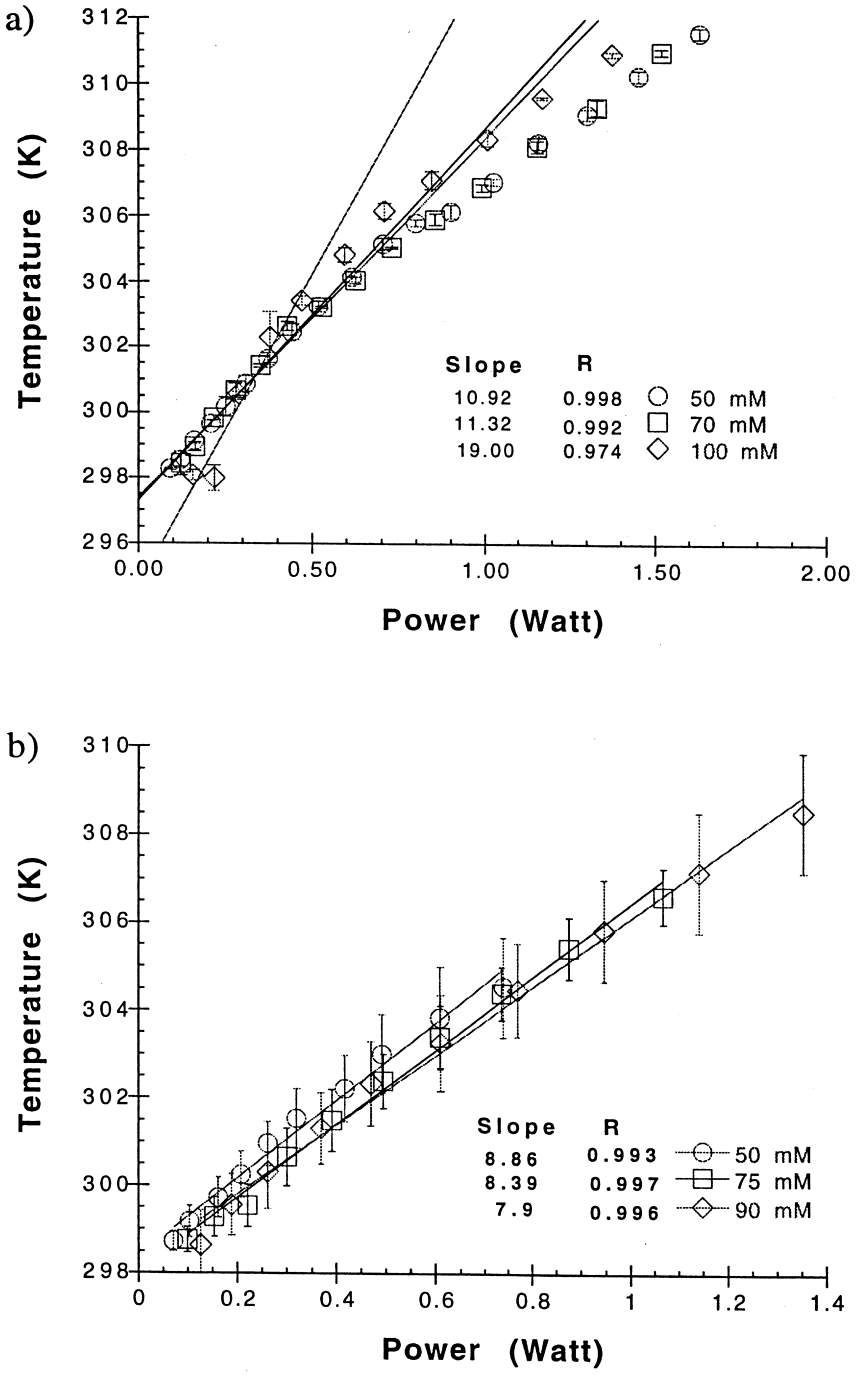

Fig. 6. Measured internal capillary temperatures as a function of power (a) aqueous and (b) formamide. Experimental conditions as in Fig. 3.

Joule heating is occurring. Although the internal capillary temperatures do not vary significantly from ambient temperature below 0.6 W (Fig. 6a), there is a distinct deviation from linearity in the temperature vs. power plots for the aqueous system which was not observed for the nonaqueous buffers.

The results of the temperature and mobility studies showed that some heating has occurred in the nonaqueous buffers; however, the amount of heat generated is not significant enough to result in the efficiency loss observed for the oligosaccharide in Fig. 4b. In contrast, there was evidence to suggest that Joule heating is occurring with the aqueous buffers above ca. 0.6 W which can contribute to the loss in efficiency in Fig. 4a.

The electroosmotic mobilities shown in Fig. 5a and b were corrected for temperature induced changes in viscosity using Eqs. (3) and (6) [9]

$$T = m(\text{Power}) + b \tag{6}$$

where m and b (K) are the slope and intercept, respectively. By utilizing Eq. (6), the internal capillary temperature (K) may be calculated for any given power over this range. The corrected mobilities in Fig. 7a and b show that heating is taking place in the aqueous and nonaqueous buffer media; however, based on all of the previous results it seems that the amount of heat generated in the nonaqueous media is small enough so that it can be effectively dissipated as opposed to the aqueous media.

Since Joule heating does not appear to be contributing to the decreased efficiencies for the oligosaccharide in the nonaqueous systems, wall adsorption and injection volume were investigated as additional sources of band broadening. One possible mechanism of adsorption is through hydrogen bonding between the –OH groups on the sugar moieties of the saccharide and the ionized silanol groups on the capillary wall. The efficiency of acetone was measured as a function of electric field strength for the aqueous and nonaqueous buffers. Acetone is assumed to have no interactions with the capillary wall at pH 9. In Fig. 8a and b, the acetone efficiency increases to a maximum in the aqueous medium and then begins on a downward trend with continued increases in voltage, whereas in the nonaqueous medium the acetone efficiency continues to increase with higher voltage. The efficiency of the oligosaccharides in the aqueous and nonaqueous media was also observed to increase to a maximum after which it decreased with continued increases in voltage. These results suggest that the saccharides may be experiencing some wall interaction. Additionally, the fact that the acetone efficiency does not decrease at the higher voltages in the nonaqueous buffer further supports the idea that Joule heating is not producing the decrease in saccharide efficiency seen in Figs. 4b. However, the slight downward trend of acetone in the aqueous medium along with the aqueous Ohm's law plot and internal capillary temperature data we concluded that Joule heating is contributing to the decreased efficiencies in Fig. 4a along with wall adsorption.

The contribution of wall adsorption to band dispersion is expressed by Eq. (7) [12]

$$H_{\text{ads}} = \left[\frac{K^2}{D} \frac{R_c}{R_c + 2K} + \frac{4K}{(R_c + 2K)k_d} \right] \upsilon_m \tag{7}$$

where H_{ads}, K, k_d, R_c, D, and υ_m are the plate height, distribution coefficient between the bulk solvent and the wall, rate constant of desorption, capillary inner radius, sample diffusion coefficient and mean sample velocity, respectively. Eq. (7) is equivalent to the C term of the Golay equation for chromatography

$$H_{\text{tot}} = \frac{B}{\upsilon} + C\upsilon \tag{8}$$

where the B and C terms represent contributions from longitudinal diffusion and resistance to mass transfer, respectively. Calculation of υ_m for maltopentaose in the aqueous and formamide media at 298 (K) gives 0.0729 and 0.0203 cm/s, respectively. The 3.6-fold greater υ_m value of the aqueous medium over that of the nonaqueous will decrease the time available for the sample to undergo the adsorb/desorb process resulting in a larger plate height. In contrast, the rate of desorption is inversely proportional to the plate height. The desorption rate is given by Eq. (9) as

$$k_d = \frac{8RT}{3\eta} \tag{9}$$

where R, T and η are the gas constant (8.3145 J K^{-1} mol^{-1}), temperature (K), and viscosity (kg m^{-1} s^{-1}), respectively [13]. Calculated values of k_d at

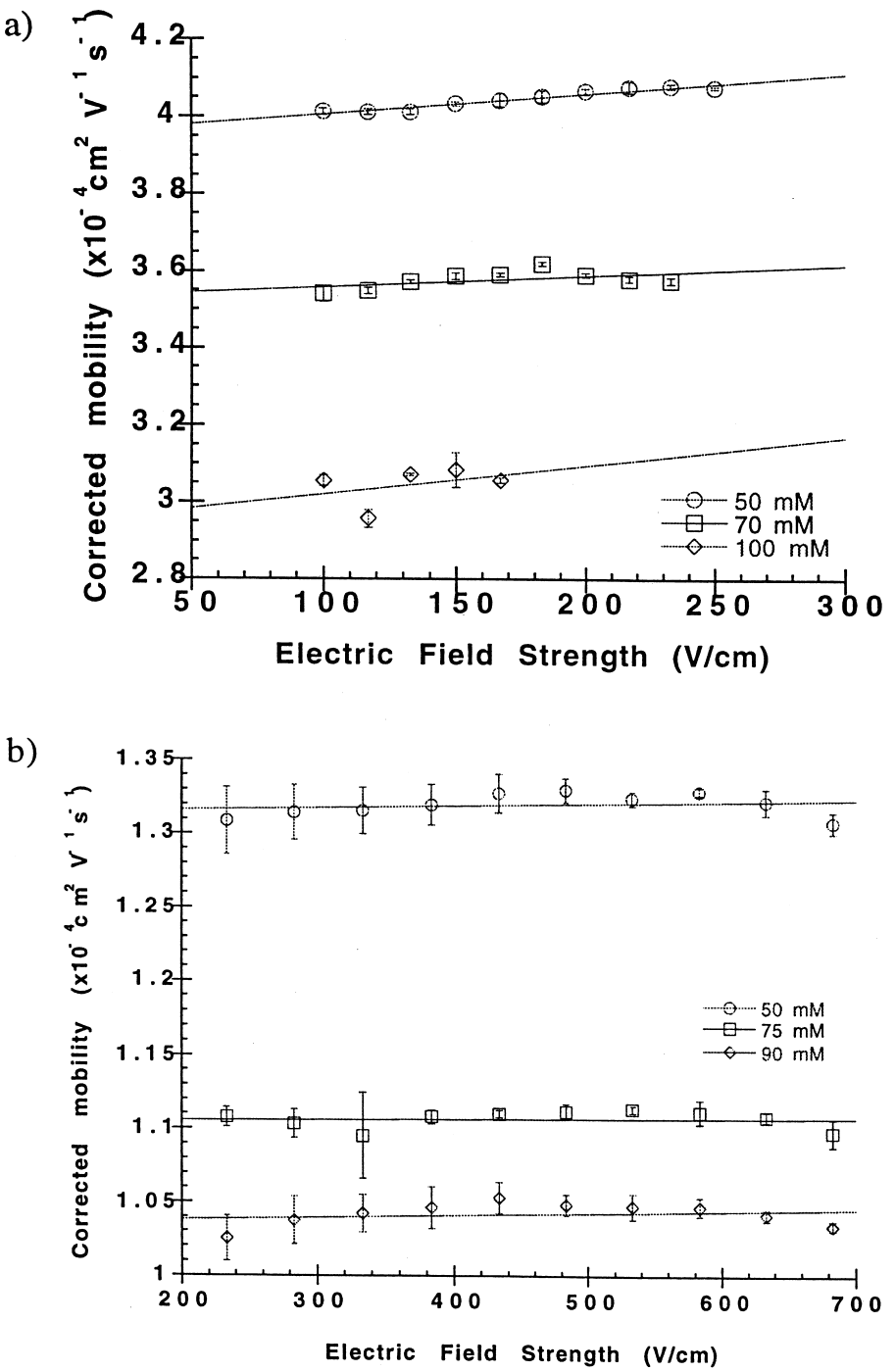

Fig. 7. Mobility data of Fig. 5 corrected for the change in viscosity with temperature. The linearity of these plots indicates that Joule heating causes the change in mobility observed in Fig. 5. Conditions as in Fig. 3.

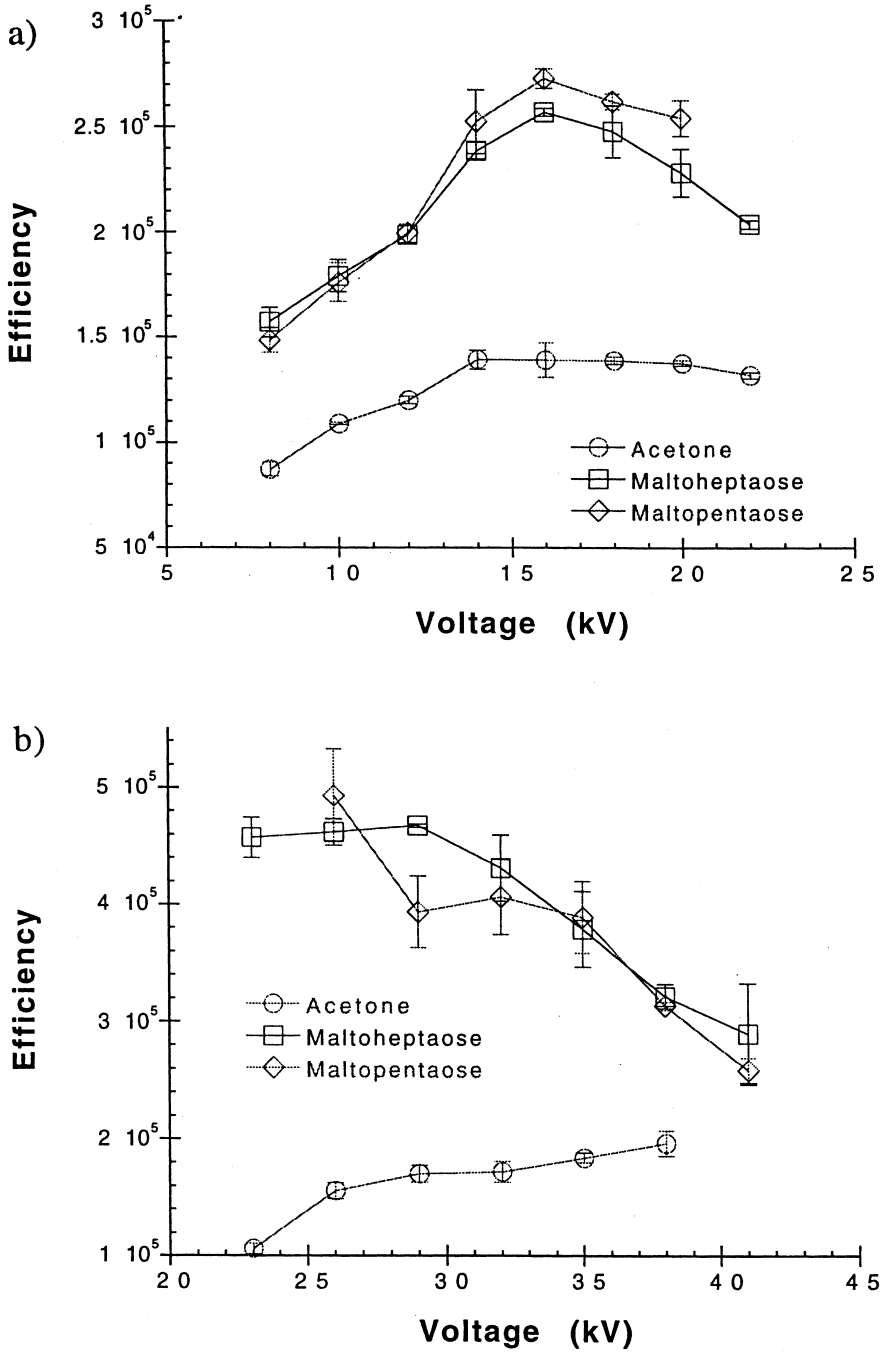

Fig. 8. Efficiency plot for (a) aqueous CE and (b) NACE. Samples include acetone and two ANTS-derivatized oligosaccharides, maltopentaose and maltoheptaose. Capillary dimensions as in Fig. 3. Buffer concentrations: 70 and 75 m*M* sodium phosphate, pH 9 for the aqueous and nonaqueous media, respectively.

298 and 306 (K) for the aqueous phase are $7.4 \cdot 10^9$, $9.06 \cdot 10^9$, and for formamide $2 \cdot 10^9$, $2.52 \cdot 10^9$ (l mol^{-1} s^{-1}), respectively. At each temperature, the rate of desorption in formamide is 3.6-fold smaller than in the aqueous medium. Lower k_d rates in the nonaqueous medium results in larger plate heights. Interestingly, the v_m and k_d values of the aqueous and nonaqueous media appear to balance each other. This tends to support the results shown in Fig. 4a and b where the maximum efficiency of the saccharide is reached at approximately the same experimental conditions for both the aqueous and nonaqueous media. The distribution coefficient (K) could not be calculated; however, the sample diffusion coefficient (D) is expected to decrease with increased viscosity, resulting in larger H_{ads} values for formamide.

The injection volume was also investigated as a possible source of band broadening. Delinger and Davis showed that the initial plug length can significantly effect efficiency at high applied voltages [6]. The authors demonstrated that at low voltages sufficient time exists for diffusion to broaden the analyte plug which results in the efficiency varying linearly with voltage. However, at high voltages the sample plug moves very rapidly down the capillary and does not have the time to broaden by diffusion. This results in the efficiency being dependent on the initial plug length of the sample instead of the voltage.

Different volumes of 0.3, 0.5, 0.99, 1.65, 1.98 and 3.3 nl of the ANTS-derivatized saccharide, maltopentaose, were injected at both a high and low voltage for the aqueous and nonaqueous buffer media. Figs. 9 and 10 show the injection volume results for the 70 mM aqueous sodium phosphate buffer at 10 and 23 kV (Fig. 9) and the 75 mM nonaqueous sodium phosphate buffer at 26 and 38 kV (Fig. 10), respectively. In Fig. 9, the saccharide efficiency was observed to decrease with an increase in injection volume at the larger voltage, and the efficiencies are overall greater at the higher voltage (23 kV) except for the 3.3 nl volume. This suggests that the volumes used in our experiments are small enough since the efficiency still appears to be increasing with the voltage. The nonaqueous results in Fig. 10 show the same types of trends with the efficiency being voltage dependent. Based on the

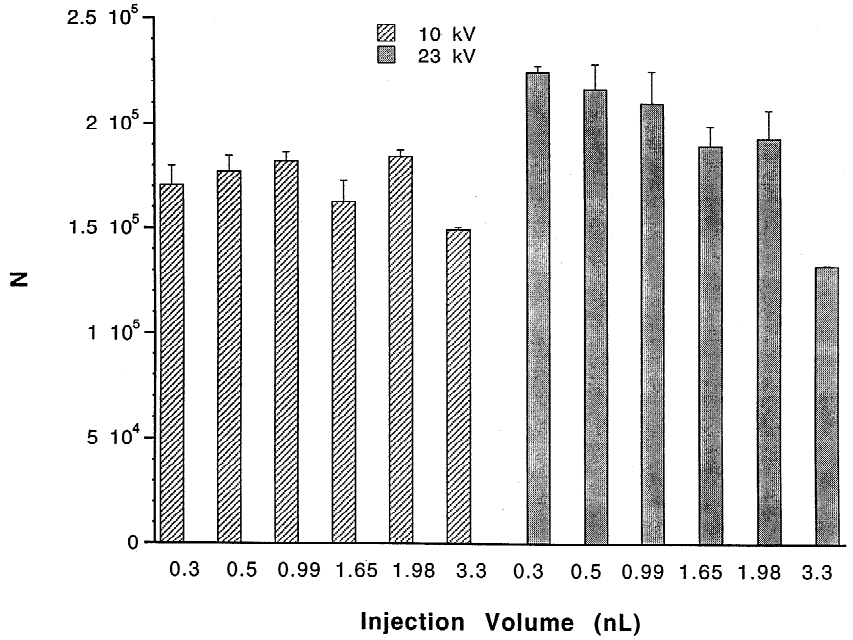

Fig. 9. Aqueous injection volume study. Buffer is 70 mM sodium phosphate at pH 9. Injection volumes: 0.3, 0.5, 0.99, 1.65, 1.98 and 3.3 nl. Capillary dimensions as in Fig. 3. Sample is ANTS-derivatized maltopentaose ($2.8 \cdot 10^{-4}$ M).

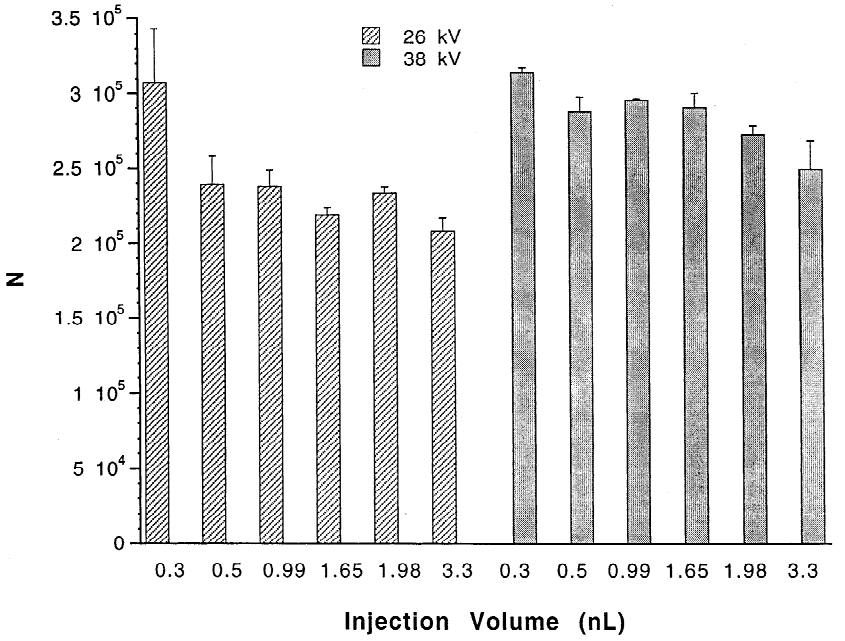

Fig. 10. Nonaqueous (formamide) injection volume study. Buffer is 75 m*M* sodium phosphate at pH 9*. Injection volumes: 0.3, 0.5, 0.99, 1.65, 1.98 and 3.3 nl. Capillary dimensions as in Fig. 3. Sample is ANTS-derivatized maltopentaose ($2.8 \cdot 10^{-4}$ *M*).

results of these studies we concluded that the injection volume of 1.61 nl used in the original efficiency studies shown in Fig. 4a and b was not causing the observed decreases in the saccharide efficiencies. Instead it was concluded that the oligosaccharides possess some affinity for the capillary wall which resulted in their decreased efficiency at higher voltages due to increased sample velocity at constant sorption kinetics.

3.3. Separation of oligosaccharide mixture

Under the operating conditions of pH 9 and positive applied voltage, the negatively charged oligosaccharides will have an electrophoretic mobility towards the injection end (anodic) of the capillary; however, the larger EOF towards the cathodic end produces a net electrophoretic migration towards the detector. Since derivatization only takes place at one point on the saccharide structure, all the saccharides in the homologous series have the same charge but different mass. The elution order is then determined by the charge-to-mass ratio with the largest saccharide (maltoheptaose) in the series eluting first and the smallest (maltose) eluting last. Electropherograms for the separation of the homologous series using aqueous CE and NACE at their respective optimum buffer concentration and applied voltage are shown in Figs. 11 and 12.

As expected, NACE produced larger efficiencies than CE; however, in Table 2 we show the unexpected reduction in efficiency for the saccharides when injected as a mixture compared to individually. The earlier eluting peaks of the mixture exhibited higher efficiencies since they spend less time on the column and therefore experience less longitudinal diffusion. Additionally, the earlier eluting peaks were the larger saccharides which inherently have smaller diffusion coefficients. This decrease in the efficiency of the saccharide mixture was further investigated by injecting a series of mixtures each containing one additional saccharide of the homologous series. The results of these studies are shown in Fig. 13. The observed decrease in efficiency was correlated with the number of saccharides in the mixture. The decreased efficiencies in the mixture were attributed to electrophoretic dispersion. The concentration of

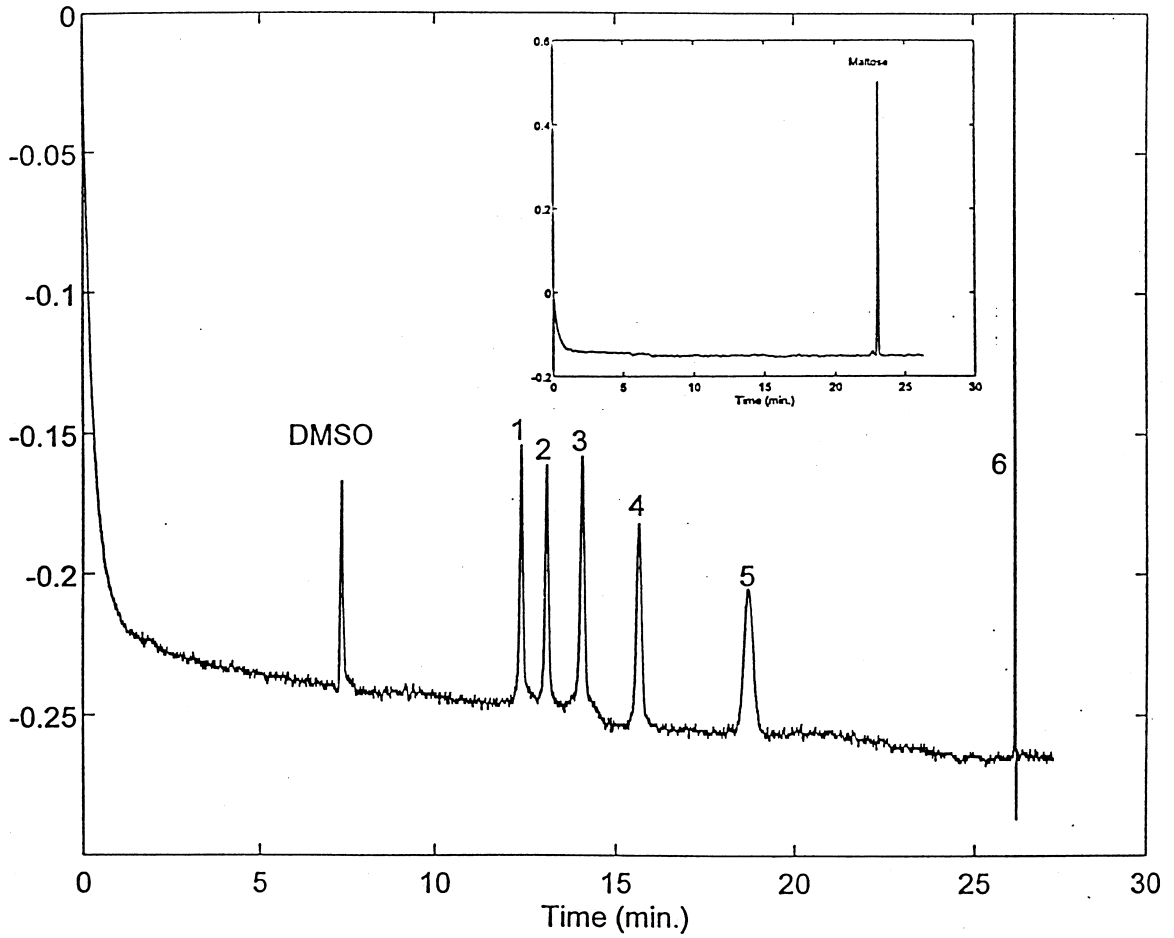

Fig. 11. Electropherogram of ANTS-derivatized maltooligosaccharides using aqueous CE at pH 9 with 70 m*M* sodium phosphate buffer. Sample separation: (1) maltoheptaose, (2) maltohexaose, (3) maltopentaose, (4) maltotetraose, (5) maltotriose and (6) maltose. CE conditions: 14 kV, 56 μA; capillary dimensions as in Fig. 3.

the individual saccharides injected was $2.64 \cdot 10^{-4}$ M; however, the mixture consisted of six saccharides each at the above concentration resulting in an ionic strength of $8.3 \cdot 10^{-3}$ *M*. Therefore, the conductivity of the mixture was increased over that of an individual saccharide which in turn could have produced enough conductivity difference between the sample and buffer zones to introduce band broadening effects due to electrophoretic dispersion.

4. Conclusion

The results of these experiments show that Joule heating occurs in the aqueous and nonaqueous media; however, the nonaqueous systems generate less heat and are therefore able to dissipate the heat as given by the linear Ohm's law plots. The viscosity of formamide decreases the mobility of the buffer ions minimizing the electrical current produced at the larger field strengths resulting in less heat being generated. Additionally, the viscosity of the formamide may be inducing some stacking effects by creating a large contrast in the electric field strength between the separation and sample zones. This phenomenon may explain why the oligosaccharides experience overall higher efficiencies in the nonaqueous media even though the retention times are longer

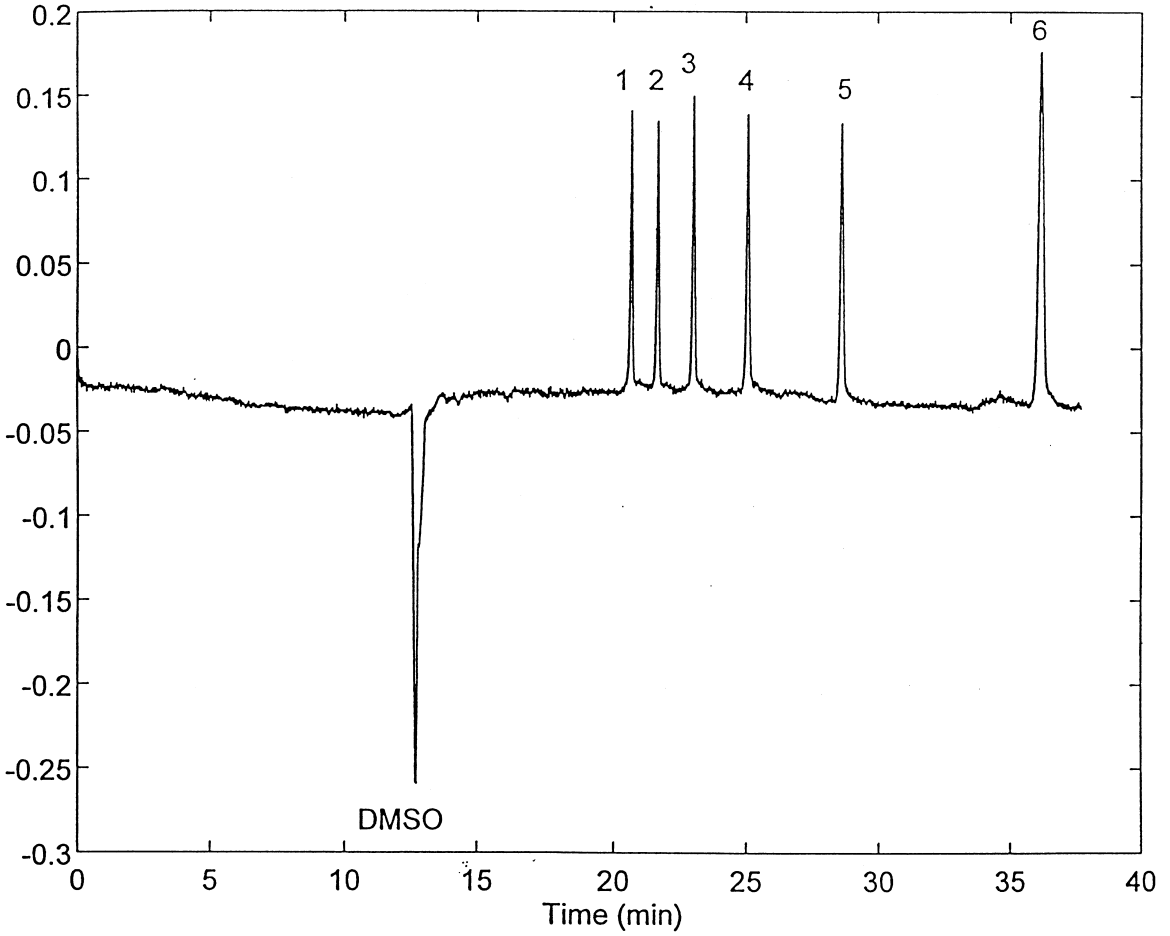

Fig. 12. Electropherogram of ANTS-derivatized maltooligosaccharides using NACE at pH 9* with 75 m*M* sodium phosphate buffer in formamide. Sample separation as in Fig. 12. CE conditions: 25 kV, 16 μA; capillary dimensions as in Fig. 3.

Table 2
Separation efficiencies for oligosaccharide mixture with NACE and CE (data are averages of three injections)

Oligosaccharide	Efficiency					
	NACE			CE		
	Individual	Mixture	% Decrease	Individual	Mixture	% Decrease
Maltoheptaose	385 397	298 092	23	226 146	90 376	60
Maltohexaose	402 160	307 861	23	200 559	85 466	57
Maltopentaose	387 743	291 150	25	175 829	73 616	58
Maltotetraose	356 725	269 674	24	137 649	58 648	57
Maltotriose	303 717	249 822	18	82 743	27 547	66
Maltose	216 046	197 411	9	236 685	4 294 247	1714[a]

[a] Percent increase.

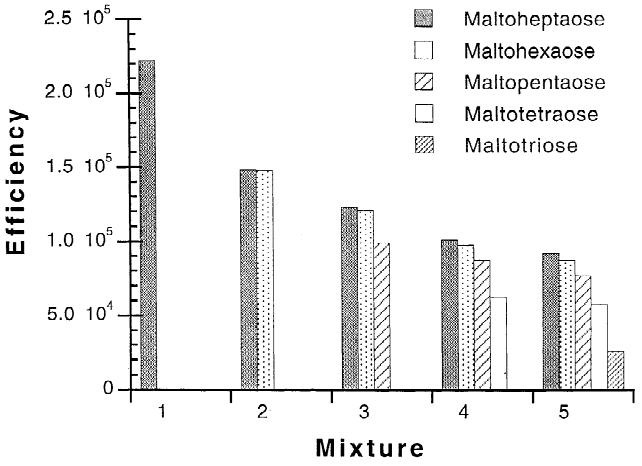

Fig. 13. Measured efficiencies for various mixtures of the ANTS-derivatized maltooligosaccharides with CE. Each mixture contains one additional saccharide. Experimental conditions as in Fig. 12.

than in the aqueous media. The overall efficiency in formamide was about 1.5-times that in the aqueous media. It was concluded that wall adsorption was the band broadening mechanism responsible for the decrease in saccharide efficiency with increased voltage above 30 kV in the nonaqueous media. The decreased oligosaccharide efficiency in the aqueous media was attributed to Joule heating as well as wall adsorption The effect of the wall adsorption on the plate height is similar to that of resistance to mass transfer in HPLC.

Acknowledgements

We gratefully acknowledge a research grant from the National Institutes of Health (GM 38738).

References

[1] J.W. Jorgenson, K.D. Lukacs, Anal. Chem. 53 (1981) 1298.
[2] E. Grushka, R.M. McCormick, J. Kirkland, Anal. Chem. 61 (1989) 241–246.
[3] X. Huang, W.F. Coleman, R.N. Zare, J. Chromatogr. 480 (1989) 95–110.
[4] J.H. Knox, Chromatographia 26 (1988) 329–337.
[5] J. Kutter, T. Welsch, J. High Resolut. Chromatogr. 18 (1995) 741–744.
[6] S.L. Delinger, J.M. Davis, Anal. Chem. 64 (1992) 1947–1959.
[7] C. Chiesa, Cs. Horváth, J. Chromatogr. 645 (1993) 337–352.
[8] P.W. Atkins, in: Physical Chemistry, 4th ed., W.H. Freeman, New York, 1990, Ch. 24.
[9] D.S. Burgi, K. Salomon, R.L. Chien, J. Liq. Chromatogr. 14 (1991) 847–867.
[10] V.I. Skomorokhov, A.F. Dregalin, J. Eng. Phys. Thermophys. 65 (1993) 1044–1046.
[11] D.R. Lide (Ed.), CRC Handbook of Chemistry and Physics, 71st ed., CRC Press, Boca Raton, FL, 1991, pp. 6–9.
[12] J.L. Miller, M.G. Khaledi (Eds.), High Performance Capillary Electrophoresis, Chemical Analysis Series, Vol. 146, Wiley, New York, 1998, Ch. 2.
[13] P.W. Atkins, Physical Chemistry, 5th ed., W.H. Freeman, New York, 1994, pp. 935–937, Ch. 27.
[14] S.S. Rachhpal, M.G. Khaledi, Anal. Chem. 66 (1994) 1141–1146.